# Polariton transport in one-dimensional channels

M. Yu. Petrov[1,*] and A. V. Kavokin[1,2]

[1]*Spin Optics Laboratory, Saint-Petersburg State University, Petrodvorets, 198504 St. Petersburg, Russia*

[2]*Physics and Astronomy School, University of Southampton, Highfield, Southampton SO17 1BJ, United Kingdom*

(Received 17 May 2013; revised manuscript received 1 July 2013; published 15 July 2013)

We study theoretically the transport of linearly polarized exciton-polaritons in a quasi-one-dimensional microcavity channel separating two polariton condensates generated by optical pumping. The direction and value of mass and spin currents are controlled by the relative phase and polarization of two condensates, as in the stationary Josephson effect. However, due to dissipation and particle-particle interactions, the current density is inhomogeneous: it strongly depends on the coordinate along the axis of the channel. A stationary spin domain can be created in the channel, its position would be sensitive to the phase difference between two bordering condensates.

DOI: 10.1103/PhysRevB.88.035308 PACS number(s): 71.36.+c, 42.55.Sa, 42.65.Pc

## I. INTRODUCTION

Exciton-polaritons are electrically neutral bosonic spin carriers. They offer a valuable alternative to the traditional spintronics based on the charged fermionic spin carriers, electrons and holes.[1–3] Recent experiments demonstrated a high potentiality of the exciton-polaritons for the ballistic transport over macroscopic distances.[4,5] Spin Josephson,[6] optical spin Hall,[7] and optical Aharonov-Bohm[8] effects based on the exciton-polaritons are widely discussed. The spin currents carried by the exciton-polaritons are being studied experimentally by the polarization-resolved microphotoluminescence.[9,10] Meanwhile, the theory of bosonic spin transport in dissipative media is far from being built. The concept of bosonic spin conductivity is not clearly established yet. The interplay between nonlinear amplification effects and dissipation induced by the radiative decay of exciton-polaritons makes building up of the theory of the polariton spin currents an interesting and nontrivial task.

This work is aimed at a theoretical description of the bosonic transport in a dissipative environment by considering the simplest model system, a one-dimensional channel. Such a system can be realized in a semiconductor microcavity with embedded quantum wells, in the regime of the strong exciton-photon coupling.[11] We shall assume that the temperature is low enough to allow for formation of a spatially coherent polariton condensate[12] able to expand over the macroscopic distances without significant dephasing, as it has been experimentally observed in Ref. 10.

A one-dimensional channel similar to those studied in fermionic systems[13] can be formed by the etching of the upper Bragg mirror of a microcavity in order to create a lateral confinement for exciton-polaritons, which would be free to move along the axis of the channel.[5,14] In contrast to the system studied in Ref. 5, where the channel has been closed on both sides, we consider an open channel connecting two semi-infinite microcavity areas in which the polariton condensates are created by quasiresonant optical pumping [see the scheme in Fig. 1(a)]. In this configuration, the chemical potentials of the polariton condensates to the left and right sides of the channel are set by the energies of two pumping beams [see Fig. 1(b)]. Moreover, the polarization and the phase of both condensates are also controlled by the pumping beams (see, e.g., Refs. 15–18).

We shall study the spin transfer through the channel separating two condensates as a function of their chemical potentials, phases, and polarizations. All these parameters can be efficiently controlled by the quasiresonant pumping. We shall account for the spin-dependent polariton-polariton interactions and the radiative decay of the polaritons everywhere in the structure, including the channel.

The paper is organized as follows. In Sec. II, we formulate a basic concept of the model based on the mean-field approach. Section III presents the results of numerical calculations of polariton currents in the channel at different boundary conditions. In the last section, we conclude on the specificity of bosonic spin transport in dissipative systems.

## II. THE MEAN-FIELD MODEL

In microcavities based on zinc-blend semiconductors like GaAs, exciton-polaritons formed by heavy-hole excitons have two allowed spin projections to the structure axis: $\sigma = \pm 1$. In a coherent system, the state of the polariton condensate can be described by a two-component order parameter $\Psi(\mathbf{r},t)$:[15] $\Psi(\mathbf{r},t) = [\psi_{+1}(\mathbf{r},t); \psi_{-1}(\mathbf{r},t)]$ where $\psi_\sigma(\mathbf{r},t)$ is the many-body wave function of the condensate of polaritons with a spin projection $\sigma$ at a position $\mathbf{r}$ and a time $t$. The dynamics of $\Psi(\mathbf{r},t)$ is described by the Gross-Pitaevskii (GP) equation.[15,16,19–26] The stationary state for the two-component wave function satisfies

$$\hbar\omega_p\psi_+(\mathbf{r}) = \left[\hat{E}_{\mathrm{LP}}(-i\nabla) + \alpha_1|\psi_+(\mathbf{r})|^2 + \alpha_2|\psi_-(\mathbf{r})|^2 + V(\mathbf{r}) - \frac{i\hbar}{2\tau}\right]\psi_+(\mathbf{r}) + F_{p+}(\mathbf{r}), \tag{1a}$$

$$\hbar\omega_p\psi_-(\mathbf{r}) = \left[\hat{E}_{\mathrm{LP}}(-i\nabla) + \alpha_1|\psi_-(\mathbf{r})|^2 + \alpha_2|\psi_+(\mathbf{r})|^2 + V(\mathbf{r}) - \frac{i\hbar}{2\tau}\right]\psi_-(\mathbf{r}) + F_{p-}(\mathbf{r}). \tag{1b}$$

Here, $\hat{E}_{\mathrm{LP}}(\mathbf{k})$ is the kinetic energy operator for the lower polariton (LP) branch, $V(\mathbf{r})$ is the position dependent external potential, $\tau$ is the polariton lifetime, $\alpha_1$ and $\alpha_2$ are the polariton-polariton interaction constants in parallel and antiparallel spin configurations, respectively, and $F_{p\sigma}(\mathbf{r})$ describes the pumping of polaritons with spin projection $\sigma$. The term $\hbar\omega_p$ in the

 

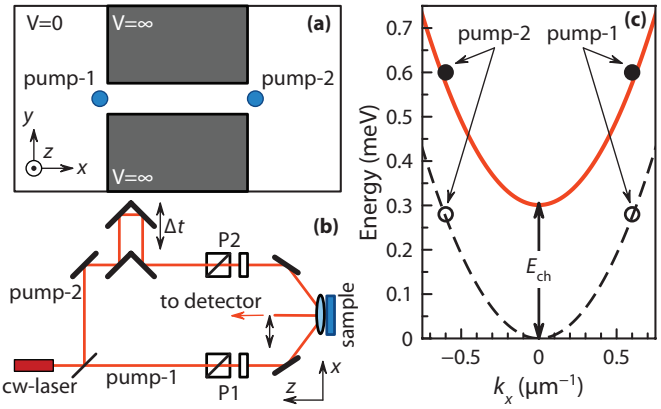


FIG. 1. (Color online) (a) Sketch showing the narrow channel defined by the spatial variation of the external potential for exciton-polaritons in a planar microcavity, $V = 0$ in the channel and $V = \infty$ in the barrier regions. Two pumping beams excite polaritons in the semi-infinite open areas near the channel ends. (b) The scheme of a model experiment, which implies that the continuous-wave laser excitation splits into two pumping beams passing through the delay line $\Delta t$ and polarizers P1 and P2. The detection system allows for collecting the spatially resolved photoluminescence signal from the channel. (c) The dispersion of the lower-polariton branch in semi-infinite open areas (dashed line) and in the channel (solid line). The pumping energy $E_p$ is tuned slightly above the lower-polariton branch energy (see Fig. 2).

left-hand side of Eqs. (1a) and (1b) sets the chemical potential of the polaritons created by pumping (we shall assume equal energies of left and right pumps).

The pumping terms that describe the quasiresonant optical injection of polaritons at the lower polariton branch at the left and right ends of the channel are introduced as follows:[19]

$$F_{p\sigma}(\mathbf{r},t) = A_\sigma\{\exp\left[-(\mathbf{r}-\mathbf{r}_L)^2/\delta^2 + i\mathbf{k}_p^L\cdot\mathbf{r}\right] + \exp\left[-(\mathbf{r}-\mathbf{r}_R)^2/\delta^2 + i\mathbf{k}_p^R\cdot\mathbf{r}\right]\}e^{-i\omega_p t}. \quad (2)$$

Here, $\mathbf{r}_L = -\mathbf{r}_R$ and $\mathbf{k}_p^L = -\mathbf{k}_p^R$ are the positions and the wave vectors of the incident light field, $\delta$ is the size of the laser-pumping spot, $A_\sigma$ is the amplitude of $\sigma$ component of the pumping field, and $\omega_p$ is the pumping frequency tuned so that $E_p = \hbar\omega_p$ is slightly above the lower-polariton branch energy [see Fig. 1(c)]. Due to the lateral confinement potential $V(\mathbf{r})$ in Eqs. (1a) and (1b), the polariton dispersion in the channel is blue shifted by $E_{\rm ch}$ with respect to the dispersion of polaritons in the semi-infinite areas to the left and right from the channel.

We solve the coupled stationary GP equations (1a) and (1b) using the Newton-type iteration procedure based on the spatial discretization with the finite element method.[27] The following parameters are used in the calculations. The channel width is $D_{\rm ch} = 5$ $\mu$m and its length is $L_{\rm ch} = 30$ $\mu$m. The lower polariton dispersion is approximated by a parabola characterized by polariton effective mass $m_{\rm LP} = 5\times10^{-5}m_0$, where $m_0$ is the mass of a free electron. The polariton lifetime is taken either $\tau = 30$ ps, which is close to the values achieved experimentally in high $Q$-factor cavities, or 300 ps, which is unrealistic in the existing semiconductor microcavities, for the sake of comparison. Polariton-polariton interaction constants $\alpha_1 = 2\times10^{-10}$ meV cm$^2$ and $\alpha_2 = -0.1\alpha_1$ are taken from Ref. 28. The coordinates of pumping spots are chosen as $y = 0$ in $x = \pm16.5$ $\mu$m. The spot size is $\delta = 0.25D_{\rm ch}$ and the wave vectors are $k_x = \pm0.6$ $\mu$m$^{-1}$. The pumping energy $E_p$ is tuned above the bare polariton branch by 0.015 meV and the amplitude $A_\sigma$ is a variable parameter.

## III. RESULTS AND DISCUSSION

We shall limit our consideration to the case of equal chemical potentials of the condensates formed at the left and right ends of the channel. We consider linearly polarized pumping beams so that $A_{+1} = A_{-1} = A$. No spin is injected to the system by the pumping lasers in this case. Let us first discuss the effect of the pumping energy $E_p$ and the pumping amplitude $A_\sigma$ on the polariton density profile in the channel. At low pumping, the nonlinear effects due to polariton-polariton interactions are negligible. In this case, the classical interference effect leads to the formation of a stationary wave with a sinusoidal profile in the channel [see Figs. 2(a) and 2(b)]. Once $A$ increases so that the nonlinear terms in Eqs. (1a) and (1b) start dominating over radiative losses, the interference pattern disappears and the polariton density in the channel becomes constant, dependent on the chemical potential set by the two pumps [see Figs. 2(c) and 2(d)]. The channel may be open or closed for the polaritons if their chemical potential is either larger or smaller than $E_{\rm ch}$, respectively [compare panels (a) versus (b) and (c) versus (d) in Fig. 2]. The most interesting and unusual bosonic spin transport phenomena are expected in the regime where $E_p > E_{\rm ch}$ and the pumping power is sufficiently large. This is the regime we are going to consider in the rest of this paper.

Let us consider now the spatial behavior of the phase of the polariton condensate in the channel. According to the conventional definition,[29] its order parameter can be represented as $\psi_\sigma(\mathbf{r}) = \sqrt{n_\sigma(\mathbf{r})}e^{iS_\sigma(\mathbf{r})}$, where $n(\mathbf{r}) = [n_+(\mathbf{r}); n_-(\mathbf{r})]$ and $S(\mathbf{r}) = [S_+(\mathbf{r}); S_-(\mathbf{r})]$ are two-component functions, which characterize the polariton density and phase, respectively. As shown above, the density profile of the ground state is almost constant along the channel axis [see Fig. 2(d)]. However, due to the dissipation, the phase of the wave function can vary as

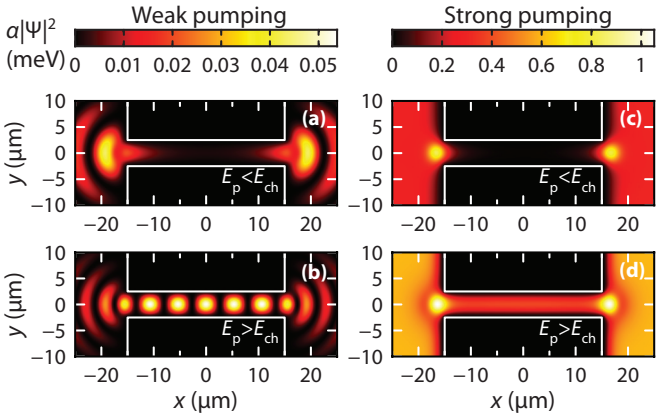


FIG. 2. (Color online) The calculated polariton density distributions in the channel in the regimes of weak pumping [(a) and (b)] and strong pumping [(c) and (d)]. The energy of the pumping beams is tuned below $E_{\rm ch}$ [(a) and (c)] and above [(b) and (d)].

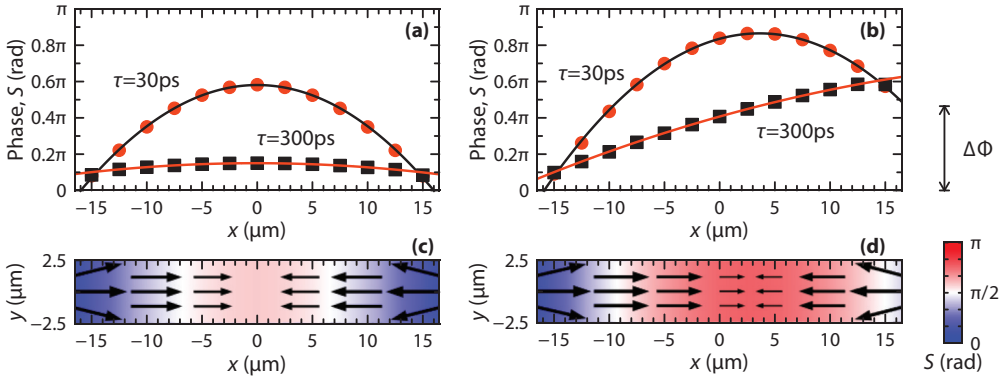


FIG. 3. (Color online) (a) and (b) The phase of the condensate in the channel $S(x)$ calculated for the different polariton lifetimes and for the different phase shifts between pumping beams (symbols). Thin lines show the fit of numerical results with Eq. (3). (c) and (d) The profiles of the phase of the condensate in the channel calculated for $\tau = 30$ ps and the same $\Delta\Phi$ as in (a) and (b), respectively. Arrows show the direction and value (in log scale) of the polariton current density.

a function of $x$. In general, it has a nearly parabolic shape as Figs. 3(a) and 3(b) show. The spatial variation of the phase can be found analytically by substituting the parabolic ansatz into the GP equation and separating its real and imaginary parts (see Appendix for details). The coordinate dependence of the phase writes

$$S(x) = -\frac{m_{\mathrm{LP}}}{6\hbar\tau}x^2 + \frac{\Delta\Phi}{L_{\mathrm{ch}}}x + S_0. \tag{3}$$

Here, $\Delta\Phi$ is the phase difference between two pumping beams governed by the time delay $\Delta t$ [see Fig. 1(b)].

As the phase profile of the order parameter is a nonlinear function of the coordinate along the axis of the channel, the current density defined as[29]

$$\mathbf{j}(\mathbf{r}) = \frac{\hbar}{m_{\mathrm{LP}}} n(\mathbf{r}) \nabla S(\mathbf{r}) \tag{4}$$

is not conserved along the channel. As $S$ is a parabolic function of the coordinate, the current density is a linear function of the coordinate. The zero current point is in the center of the channel if the phases of two condensates coincide. It can be shifted from the center to the left or right side by changing the phase difference, $\Delta\Phi$, between two condensates.

The most interesting effect occurs if the phase shift between the left and right condensates is large, i.e., $|\Delta\Phi| > L_{\mathrm{ch}}^2 m_{\mathrm{LP}}/(12\hbar\tau)$. The polariton flows become unstable: two solutions of the GP equations (1a) and (1b) have been found in this case [see Fig. 4(a)]. The first one [circles in Fig. 4(a)] corresponds to a strong variation of the density profile as it is shown in Fig. 4(b). The second one [squares in Fig. 4(a)] allows for a weaker spatial variation of the phase of the condensate. In order to maintain the phase difference $\Delta\Phi$ between two ends of the channel, the dependence $S(x)$ bounces by $\pi$ in the middle point. The phase jump corresponds to the break in the condensate profile, which is seen in Fig. 4(c). The position of the "hole" in the polariton density of a given spin component is sensitive to $\Delta\Phi$.

This fragmentation effect manifests the spontaneous pattern formation in a nonlinear bosonic system. Similar effects have been observed in polariton condensates excited in planar cavities by nonresonant optical pumping with an elliptically polarized light.[30] Manni *et al.* (see Ref. 30) observed a single-energy condensed state featuring a density and polarization pattern detectable in the polarization-resolved photoluminescence. Also, in the microcavity stripes,[5] the standing-wave states have been observed, which manifest themselves by patterns in near-field photoluminescence spectra.

In our case, however, there is no standing wave along the channel. The effect predicted here is a consequence of the destructive interference of two polariton fluids coming from the opposite ends of the channel, in a nonlinear regime.

Further nontrivial effects may be observed if the polarizations of two pumps do not coincide. As an example, we consider pumping with two linearly polarized laser beams having orthogonal polarization planes. Figures 5(a)–5(d) demonstrate the density profile of the condensate and the corresponding spatial distribution of the circular polarization degree. The circular polarization degree of the condensate is

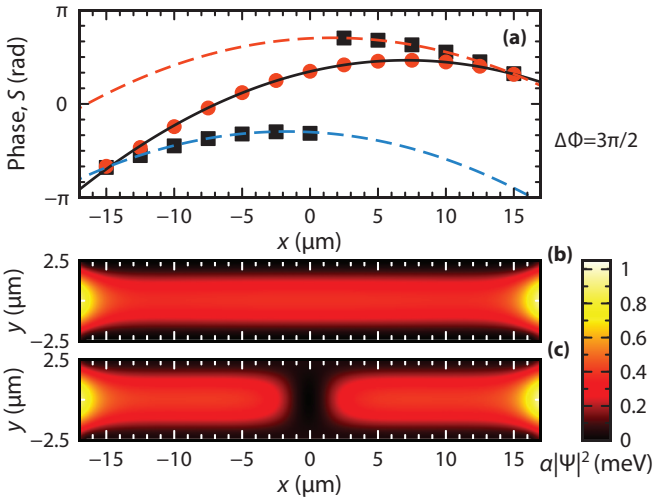


FIG. 4. (Color online) (a) The polariton phase profiles along the axis of the channel calculated at $\Delta\Phi = 3\pi/2$ (symbols) and their parabolic fits with Eq. (3) (lines). (b) and (c) The corresponding density profiles of the components of the condensate. The color bar shows the scale of the corresponding blue shift.

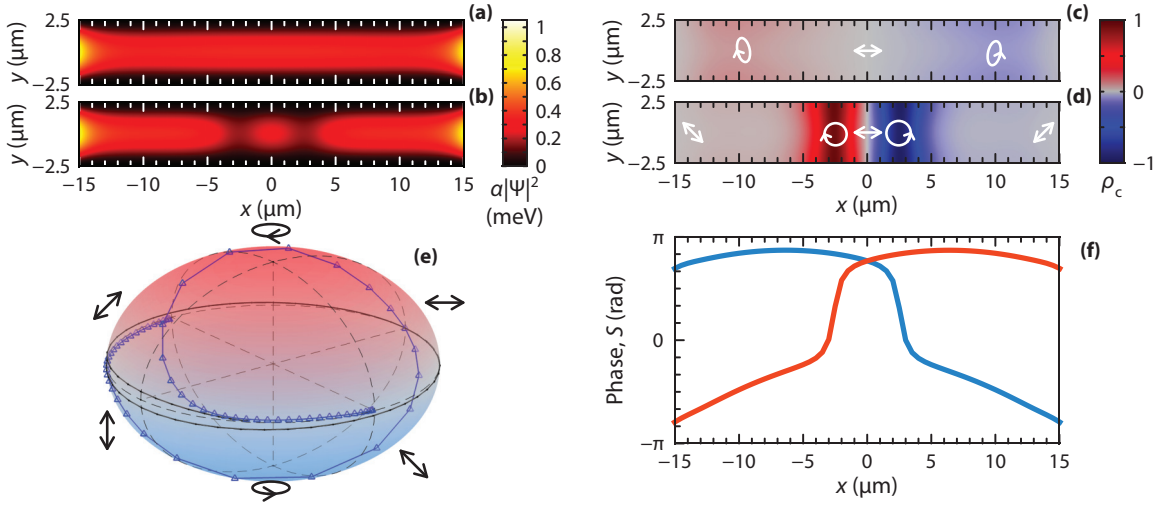


FIG. 5. (Color online) Polariton density distribution in the channel calculated for zero phase shift between right and left pumping beams $\Delta\Phi = 0$ (a) and for $\Delta\Phi = \pi$ (b). (c) and (d) The profiles of the circular polarization degree corresponding to the density distributions shown in (a) and (b). Arrows indicate orientations of the Stokes vector of the condensate at different points along the axis of the channel at $y = 0$. (e) The evolution of the Stokes vector on a Poincaré sphere as one goes along the axis of the channel between its left and right ends. The dotted (black) line corresponds to $\Delta\Phi = 0$ and the triangled (blue) line corresponds to $\Delta\Phi = \pi$. (f) The phase profile of the order parameter components calculated along the channel axis at $y = 0$ for $\Delta\Phi = \pi$.

defined as

$$\rho_c = \frac{|\psi_+|^2 - |\psi_-|^2}{|\psi_+|^2 + |\psi_-|^2}. \tag{5}$$

One can see that the density profile of the order parameter remains uniform along the channel. However, due to the interference of two linearly polarized waves, a domain of circular polarization is formed in the middle of the channel. In the nonlinear regime, this effect is strongly modified due to attraction of polaritons having opposite spins, which is accounted for in the GP equations by the terms proportional to $\alpha_2$. The polarization and spin distribution in the channel are described by variation of the Stokes vector of the polariton condensate along the axis of the channel. The trajectory of the Stokes vector on a Poincaré sphere calculated along the $x$ axis ($y = 0$) is shown in Fig. 5(e).

If the pumping beams have exactly opposite phases, the order parameter patterning appears right in the center of the channel. A bright spot appears between two dark areas [see Fig. 5(b)]. This effect is very clearly seen in the circular polarization degree profile [see Fig. 5(d)]. The stationary domains of left- and right-circular polarizations are clearly seen in this regime. The domains may be shifted along the axis of the channel by changing the phase difference between two bordering condensates.

The circular polarization domains (spin domains) are formed if the fragmentation of the polariton density occurs at the locations placed symmetrically around $x = 0$. The break in polariton density for one of the spin components is accompanied by the phase jump by $\pi$ as it is shown in Fig. 5(d). At the same time, in the opposite polarization, the signal varies smoothly. The appearance of circular polarization domains manifests separation of phases in the spinor bosonic system. This effect may be seen as a topological transition in a driven and dissipative nonlinear system. Experimentally, the spin domains may be detected by near-field photoluminescence. The positions of domain walls are strongly sensitive to the phase shift $\Delta\Phi$. In particular, the deviation of $\Delta\Phi$ from $\pm\pi$ points by $\pi/6$ shifts the circular domains by a half of their size. Increasing further the phase difference between two pumps one destroys the domain structure.

## IV. SUMMARY

To summarize, we have studied theoretically the polariton mass and spin transport in a one-dimensional microcavity channel. We have shown that in the stationary regime, under continuous-wave quasiresonant excitation by two pumping beams, the polariton current in the channel is sensitive to the energy and intensity, relative phase, and polarization of the pumping beams. In the nonlinear regime, we have found that the value and direction of polariton currents varies along the axis of the channel. The polariton flow is found to be very sensitive to the phase difference between pumping beams. At the phase differences between two pumps close to $\pm\pi$, the fragmentation of the condensate takes place. If the two pumps have orthogonal linear polarizations, the spin domains appear.

## ACKNOWLEDGMENTS

We thank K. V. Kavokin and I. V. Ignatiev for useful discussions. M.Y.P. acknowledges support of Computer Center of Saint-Petersburg State University providing with the software. The financial support from the Russian Ministry of Education and Science (Contract No. 11.G34.31.0067) is acknowledged.

## APPENDIX: DERIVATION OF EQ. (3)

To derive the coordinate dependence of the phase profile of the polariton wave function given by Eq. (3), one can use a simplified 1D model. In this case, by applying the Madelung

transformation of the wave function $\psi_\pm = \sqrt{n_\pm} e^{iS_\pm}$ and by substituting it into the GP equations (1a) and (1b), one easily obtains a system of two interconnected differential equations for real and imaginary parts of the order parameter. The imaginary part is described by a continuity equation

$$-\frac{\hbar}{m}(\nabla n_\pm \nabla S_\pm + n_\pm \nabla^2 S_\pm) = \frac{n_\pm}{\tau}. \tag{A1}$$

Assuming that the density of the polaritons smoothly varies along the channel, we neglect the quantum pressure term (Thomas-Fermi limit) in the real part of the GP equation. It writes

$$\frac{\hbar^2}{2m}(\nabla S)^2 + \alpha_1 n_\pm + \alpha_2 n_\mp = \hbar\omega_p. \tag{A2}$$

As we are interested here only in the dependence of functions $n_\pm$ and $S_\pm$ on $x$ coordinate, we substitute them by parabolic functions

$$S_\pm = S_2^\pm x^2 + S_1^\pm x + S_0^\pm, \tag{A3a}$$

$$n_\pm = n_2^\pm x^2 + n_1^\pm x + n_0^\pm. \tag{A3b}$$

Additionally, the pumping defines the boundary condition

$$S_\pm\left(\frac{L_{\rm ch}}{2}\right) - S_\pm\left(-\frac{L_{\rm ch}}{2}\right) = \Delta\Phi, \tag{A4}$$

from which $S_1^\pm = \Delta\Phi/L_{\rm ch}$. The remaining coefficients can be found by substituting Eqs. (A3a) and (A3b) into Eqs. (A1) and (A2) and by equating the factors at equal powers.

*m.petrov@spbu.ru


[1] I. A. Shelykh, K. V. Kavokin, A. V. Kavokin, G. Malpuech, P. Bigenwald, H. Deng, G. Weihs, and Y. Yamamoto, Phys. Rev. B **70**, 035320 (2004).

[2] I. A. Shelykh, A. V. Kavokin, Y. G. Rubo, T. C. H. Liew, and G. Malpuech, Semicond. Sci. Technol. **25**, 013001 (2010).

[3] I. Carusotto and C. Ciuti, Rev. Mod. Phys. **85**, 299 (2013).

[4] C. Leyder, M. Romanelli, J. P. Karr, E. Giacobino, T. C. H. Liew, M. M. Glazov, A. V. Kavokin, G. Malpuech, and A. Bramati, Nat. Phys. **3**, 628 (2007).

[5] E. Wertz, L. Ferrier, D. D. Solnyshkov, R. Johne, D. Sanvitto, A. Lemaître, I. Sagnes, R. Grousson, A. V. Kavokin, P. Senellart, G. Malpuech, and J. Bloch, Nat. Phys. **6**, 860 (2010).

[6] G. Pavlovic, G. Malpuech, and I. A. Shelykh, Phys. Rev. B **87**, 125307 (2013).

[7] A. Kavokin, G. Malpuech, and M. Glazov, Phys. Rev. Lett. **95**, 136601 (2005).

[8] I. A. Shelykh, G. Pavlovic, D. D. Solnyshkov, and G. Malpuech, Phys. Rev. Lett. **102**, 046407 (2009).

[9] A. Amo, T. C. H. Liew, C. Adrados, R. Houdre, E. Giacobino, A. V. Kavokin, and A. Bramati, Nat. Photon. **4**, 361 (2010).

[10] C. Adrados, T. C. H. Liew, A. Amo, M. D. Martín, D. Sanvitto, C. Antón, E. Giacobino, A. Kavokin, A. Bramati, and L. Viña, Phys. Rev. Lett. **107**, 146402 (2011).

[11] A. V. Kavokin, J. J. Baumberg, G. Malpuech, and F. P. Laussy, *Microcavities* (Oxford University, New York, 2007).

[12] J. Kasprzak, M. Richard, S. Kundermann, A. Baas, P. Jeambrun, J. M. J. Keeling, F. M. Marchetti, M. H. Szymańska, R. André, J. L. Staehli, V. Savona, P. B. Littlewood, B. Deveaud, and Le Si Dang, Nature (London) **443**, 409 (2006).

[13] T. J. Thornton, M. Pepper, H. Ahmed, D. Andrews, and G. J. Davies, Phys. Rev. Lett. **56**, 1198 (1986).

[14] T. Gao, P. S. Eldridge, T. C. H. Liew, S. I. Tsintzos, G. Stavrinidis, G. Deligeorgis, Z. Hatzopoulos, and P. G. Savvidis, Phys. Rev. B **85**, 235102 (2012).

[15] N. A. Gippius, I. A. Shelykh, D. D. Solnyshkov, S. S. Gavrilov, Y. G. Rubo, A. V. Kavokin, S. G. Tikhodeev, and G. Malpuech, Phys. Rev. Lett. **98**, 236401 (2007).

[16] T. C. H. Liew, A. V. Kavokin, and I. A. Shelykh, Phys. Rev. Lett. **101**, 016402 (2008).

[17] D. Sarkar, S. S. Gavrilov, M. Sich, J. H. Quilter, R. A. Bradley, N. A. Gippius, K. Guda, V. D. Kulakovskii, M. S. Skolnick, and D. N. Krizhanovskii, Phys. Rev. Lett. **105**, 216402 (2010).

[18] T. K. Paraïso, M. Wouters, Y. Léger, F. Morier-Genoud, and B. Deveaud-Plédran, Nat. Mat. **9**, 655 (2010).

[19] I. Carusotto and C. Ciuti, Phys. Rev. Lett. **93**, 166401 (2004).

[20] N. G. Berloff, Phys. Rev. Lett. **94**, 010403 (2005).

[21] M. Wouters and I. Carusotto, Phys. Rev. Lett. **99**, 140402 (2007).

[22] G. Malpuech, D. D. Solnyshkov, H. Ouerdane, M. M. Glazov, and I. Shelykh, Phys. Rev. Lett. **98**, 206402 (2007).

[23] I. A. Shelykh, D. D. Solnyshkov, G. Pavlovic, and G. Malpuech, Phys. Rev. B **78**, 041302(R) (2008).

[24] A. Amo, J. Lefrère, S. Pigeon, C. Adrados, C. Ciuti, I. Carusotto, R. Houdré, E. Giacobino, and A. Bramati, Nat. Phys. **5**, 805 (2009).

[25] M. Wouters, T. C. H. Liew, and V. Savona, Phys. Rev. B **82**, 245315 (2010).

[26] H. Flayac, D. D. Solnyshkov, and G. Malpuech, Phys. Rev. B **83**, 045412 (2011).

[27] COMSOL MULTIPHYSICS v4.2 has been used for numerical solution of coupled GP equations given by Eqs. (1a) and (1b). The second-order Lagrange finite elements on the triangular mesh with 0.1 $\mu$m of lateral element size have been used. Fine tuning of the nonlinear solver allows us to achieve convergence error in the order of $10^{-4}$ to ensure numerical stability of the solution.

[28] M. Vladimirova, S. Cronenberger, D. Scalbert, M. Nawrocki, A. V. Kavokin, A. Miard, A. Lemaître, and J. Bloch, Phys. Rev. B **79**, 115325 (2009).

[29] L. P. Pitaevskii and S. Stringari, *Bose-Einstein Condensation* (Clarendon, Oxford, 2003).

[30] F. Manni, K. G. Lagoudakis, T. C. H. Liew, R. André, and B. Deveaud-Plédran, Phys. Rev. Lett. **107**, 106401 (2011).